



## A New Objective Evaluation Index for Despeckled SAR Images

H. Markarian<sup>1</sup>, M. Nejati-Jahromi<sup>2\*</sup>

<sup>1</sup> Department of Electrical Engineering, Islamic Azad University South Tehran Branch, Tehran, Iran.

<sup>2</sup> Department of Electrical Engineering, Shahid Sattari Aeronautical University of Science and Technology Tehran, Iran.

**ABSTRACT:** Synthetic aperture radar (SAR) images due to the usage of coherent imaging systems are affected by speckle. Thus, lots of despeckling filters have been introduced up to now to suppress the speckle. Hence, objective and subjective evaluations of the denoised SAR images become necessity. Many objective evaluating estimators have been introduced to evaluate the performance of despeckling filters. However, two main problems exist when evaluating the SAR images: 1) contradiction of objective and subjective evaluations and 2) absence of the ground-truth (noiseless) SAR image of the illuminated scene. Lots of efforts had been made to introduce precise referenceless estimators for SAR images which will be compatible with subjective evaluation and the results obtained by other estimators. In this paper, we propose a new edge detector and also a new referenceless estimator called “Extended Ratio Edge Detector” and “ $E-\alpha\beta$ ”, respectively. These algorithms are the extended version of “Ratio Edge Detector” and “ $\alpha\beta$ ” estimator. Experiments on images obtained from RADARSAT-1 dataset showed that the proposed edge detector and the estimator outperform their previous versions of algorithms as the proposed  $E-\alpha\beta$  parameter subjectively reports up to 0.2 better results for images filtered with FANS filter in comparison with other used methods. This is also validated by  $\beta_{ratio}$  and  $\mu_{ratio}$  parameters. Therefore, it is a reliable tool for objective evaluation of despeckled SAR images.

### Review History:

Received: 25 February 2018

Revised: 19 July 2018

Accepted: 11 September 2018

Available Online: 18 September 2018

### Keywords:

Synthetic Aperture Radar (SAR)

Despeckling

Edge Detection

Objective Evaluation

### 1- Introduction

SAR systems are able to operate during day or night and under all weather conditions, so they are used for a wide variety of applications [1] such as environmental monitoring, earth-resource mapping and military systems. As it is known, any coherent imaging system such as laser [2], ultrasound [3], synthetic aperture sonar [4] and SAR [5], works with the processing of backscattered signals which cause that the generated image is affected with multiplicative noise named speckle [6]. In signal and image processing point of view, speckle is not really a noise, as it provides useful information. However, speckle reduces the image visual quality and, thus, causes problems when interpreting the images. So, elimination of the speckle becomes a necessity in coherent imaging systems, especially in SAR systems where high precision of the illuminated scene is desired.

Up to now, a lot of despeckling filters and techniques such as geometric filters [7], adaptive filters [8-10], multi-temporal filters [11], variational methods based on partial differential equations (PDE) [12, 13] and MAP [14-16] have been introduced for SAR systems. Objective evaluation of the despeckling filters, is done by using some image quality indexes such as Equivalent Number of Looks (ENL) [17], Structural Similarity Index (SSIM) [18],  $\beta$ -correlator [19] and Peak Signal to Noise Ratio (PSNR) [20]. For accurate evaluation of the filtered images by using the image quality indexes, the ground-truth (noiseless) version of the image is required which is not available in some cases such as SAR imaging systems. For such cases, the estimation of image mean preservation and variance reduction, estimated

in a homogeneous area, are mandatory. Another solution is to use the combination of statistical quality-indexes to define the ENLs, which must be as high as possible for the denoised image. Higher ENL values indicate stronger speckle suppression. However, sometimes the objective evaluating estimators does not confirm the subjective evaluation of the filtered images; for example in [21] it is seen that although the filtered SAR images with the proposed MAP High-TV method have better results than those with the MAP-MIDAL method, the obtained ENL values for the later one is higher. Encountering these problems made the researchers introduce more precise referenceless estimators for SAR images where the use of ratio images (ratio between original noisy SAR image and filtered one) and estimation of ENL in a homogeneous area within the ratio image are becoming common [22]-[24]. Ratio images are used because in an ideal filtering operation, the ratio should show the features of pure speckle in regions where speckle is fully developed [19]. Therefore, having mean value equal to 1 in ratio images is equivalent to having ideal speckle suppression.

Recently, a new referenceless estimator, named  $\alpha\beta$ , which uses ratio images for evaluation was introduced in [25]. Although, they did not used state of art filtering methods introduced for SAR images to show the effectiveness of the new estimator, it showed a great potential in precise evaluation of the filtered SAR images which they had used in their experiments. Furthermore, they used standard ratio edge detector in  $\alpha\beta$  estimation for edge detection in ratio images which is unable to detect all the small edges appearing in the ratio image. So, in result it makes the  $\alpha\beta$  estimator fail to precisely evaluate the despeckled SAR images. Motivated

Corresponding author, E-mail: m\_nejati@azad.ac.ir

by this, in this paper we are going to propose a new ratio edge detector and thereby a new estimator to enhance the effectiveness of  $\alpha\beta$  estimator using high-order total variation (HTV) [26].

The organization of the paper is as it follows. In Section 2,  $\beta$ ,  $\beta_{ratio}$  and “Ratio Edge Detector” will be reviewed briefly. In Section 3 the proposed “Extended Ratio Edge Detector” and also  $E-\alpha\beta$  will be presented. Section 4 contains experimental results both on synthetic and real SAR images and finally in Section 5 the paper is concluded.

**2- Background**

In this section, we are going to review the  $\beta$ ,  $\beta_{ratio}$  and “Ratio Edge Detector” estimators which are used in the proposed method.

**2- 1-  $\beta$  edge estimator**

As it is known, in denoising missions, especially for SAR images, edge preservation is one of the main concerning issues.  $\beta$  edge estimator is a powerful tool which evaluates the edge preservation of the filtered image. Suppose  $I$  is the ground-truth image and  $\hat{I}$  is the filtered version of  $I$ , then  $\beta$  is defined as it follows,

$$\beta = \frac{\Gamma(\Delta I - \overline{\Delta I}, \Delta \hat{I} - \overline{\Delta \hat{I}})}{\sqrt{\Gamma(\Delta I - \overline{\Delta I}, \Delta I - \overline{\Delta I})} \times \sqrt{\Gamma(\Delta \hat{I} - \overline{\Delta \hat{I}}, \Delta \hat{I} - \overline{\Delta \hat{I}})}} \quad (1)$$

where  $\Gamma(I_1, I_2)$  is given by

$$\Gamma(I_1, I_2) = \sum_{i=1}^K I_1 \cdot I_2 \quad (2)$$

Here,  $K$  is the total number of pixels in images,  $\Delta I$  and  $\Delta \hat{I}$  are the high-pass filtered version of the images  $I$  and  $\hat{I}$  respectively, obtained with an edge detector such as Canny edge detector and also  $\overline{\Delta I}$  and  $\overline{\Delta \hat{I}}$  are the average value of their corresponding images.

As far as in SAR images, the ground-truth image due to the inherent noise added to the received data while capturing the images is not available, the ratio version of  $\beta$ , say  $\beta_{ratio}$  [25], could be used in which  $I$  and  $\hat{I}$  are replaced with noisy and ratio images respectively.  $\beta_{ratio}$  ranges between 0 and 1, where 0 implies ideal edge preservation.

**2- 2- Standard ratio edge detector**

An ideal filtering operation implies that in areas where speckle is fully developed the ratio should have the features of pure speckle, and there must be no geometric content. As far as

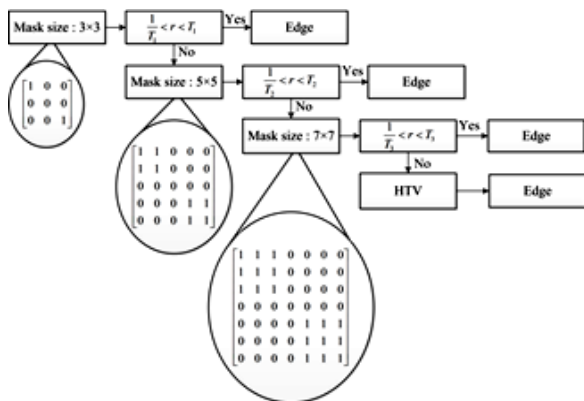


**Fig. 1. The block diagram of Extended Ratio Edge Detector using right oblique direction masks**

there is no filter which has ideal results, there always exists some geometric content in every ratio image. To extract the geometric content, several methods such as statistical analysis of the ratio image under various probability density function (pdf) distributions, histogram and texture analysis have been introduced up to now. However, no good results were obtained. Between all these methods, the “Edge Detector” [27] showed to be more effective and was applied to SAR images for years. Recently in [25], the authors used it in  $\alpha\beta$  estimation for SAR images. They used ratio images to evaluate edge preservation in the filtered SAR images; therefore they named it ratio edge detector [25]. The ratio edge detector at the neighborhood of pixel  $n$  is calculated as it follows,

$$R_n = X_1 / X_2, \quad (3)$$

where  $X_1$  and  $X_2$  are the average pixel values of two neighborhoods on opposite sides of the points, i.e. vertical, horizontal, oblique right, and oblique left. The following criterion is used to decide whether the analyzed pixel  $n$  is an edge or a homogenous region.

$$\text{pixel } n = \begin{cases} \text{edge} & , R_n < T_1 \text{ or } R_n > T_2, \\ \text{homogeneous} & , \text{else.} \end{cases} \quad (4)$$

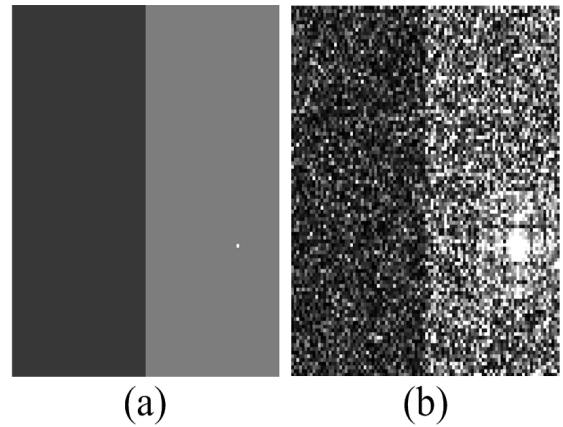


**Fig. 2. Synthetic SAR Phantom, (a) original and (b) noisy images**

Here,  $T_1$  and  $T_2$  are threshold values which depend to the number of looks of the image and usually are obtained by running the edge detector algorithm few times. In fact, to detect the most of the structure content within the ratio image, the edge detector should be performed several times using different mask sizes (usually  $3 \times 3$ ,  $5 \times 5$  and  $7 \times 7$ ) as it was used in [25]. For small mask size, a small value for  $T$  is chosen (around 0.1), then it is increased for bigger mask sizes [25]. However, again some of the contents remain undetected. In the next section, we are going to introduce a new version of ratio edge detector, called “Extended Ratio Edge Detector” which is able to detect the most of the contents in ratio images and thereby a new version of  $\alpha\beta$  estimator called “Enhanced  $\alpha\beta$ ” ( $E-\alpha\beta$ ) will be introduced.

**3- Proposed method**

As mentioned in previous section, to have better edge detection results, the ratio edge detector should be performed several times using different mask sizes (usually  $3 \times 3$ ,  $5 \times 5$  and  $7 \times 7$ ). In addition, it must be applied in all possible directions, which makes it time-consuming specially for large-sized

SAR images.

Some of the small edges remain undetected. The mentioned problems could be easily overcome by just adding one more step to the end of edge detection algorithm (see Fig. 1), i.e. the usage of high-order total variation (HTV) [26] defined as,

$$|D^2 I| = \sqrt{I_{xx}^2 + I_{yy}^2 + I_{yx}^2 + I_{xy}^2} \quad (5)$$

where  $D^2 I$  is the Hessian of image  $I$ , and  $I_{xx}^2$ ,  $I_{xy}^2$ ,  $I_{yx}^2$  and  $I_{yy}^2$  are the second order difference matrices in azimuth and range directions.

By adding HTV, there is no need to run the algorithm in all directions. So, it is possible to choose one of the oblique directions (right or left) and run the extended version of ratio edge detector algorithm, being sure that the most of the edges (including the smallest ones) are detected. Fig. 1 shows the block diagram of the extended ratio edge detector algorithm using three edge detector masks. Note that this algorithm is very similar to its previous version named ratio edge detector. Using the extended ratio edge detector, the  $E - \alpha\beta$  estimator is defined as it follows,

$$E - \alpha\beta = \{\alpha \cdot |\delta_{ENL}| + (1 - \alpha) \cdot |\delta_\mu|\} + \beta_{ratio}, \quad (6)$$

where  $\alpha \in [0, 1]$ , and  $\delta_{ENL} = ENL_{noisy} - ENL_{ratio}$ , and  $\delta_\mu = 1 - \mu_{ratio}$  are  $ENL$  and mean value of the speckle residues, respectively. In the ideal filtering of SAR images,  $ENL_{ratio}$  and  $ENL_{noisy}$ , and also  $\mu_{ratio}$  and  $\mu_{noisy}$  would be equal. Therefore,  $\delta_{ENL}$  and  $\delta_\mu$  would be zero; so the  $E - \alpha\beta$  value would be equal to  $\beta_{ratio}$ . To conclude, lower values of  $E - \alpha\beta$  means having better edge preservation when filtering a SAR image. Then the ideal filtering value for  $E - \alpha\beta$  will be zero.

The computation of  $E - \alpha\beta$  algorithm could be summarized as it follows.

$E - \alpha\beta$ Algorithm	
Initialization	
U:	Noisy image
V:	Denoised image
R=U/V :	Ratio Image
ROI <sub>noisy</sub> :	Homogeneous region in the noisy image
ROI <sub>ratio</sub> :	Homogeneous region in the ratio image
$T_1, T_2, T_3$ :	Threshold values
$\alpha$ :	weighting coefficient
Algorithm	
Extract edges of noisy image:	
1) NoisyEdge=ExtendedRatioEdgeDetector(U, $T_1, T_2, T_3$ );	
Extract edges of ratio image:	
2) RatioEdge=ExtendedRatioEdgeDetector(R, $T_1, T_2, T_3$ );	
3) Estimate $\beta_{ratio}$ for NoisyEdge and RatioEdge obtained in step 1 and 2;	
4) Estimate $\mu_{ratio}$ for ROI <sub>ratio</sub> (mean value of ROI <sub>ratio</sub> ).	
5) Estimate $\sigma_{ratio}$ for ROI <sub>ratio</sub> (variance of ROI <sub>ratio</sub> );	
6) Estimate $ENL_{ratio}$ for ROI <sub>ratio</sub> ;	
7) Obtain $E - \alpha\beta$ using Eq. (6)	

#### 4- Experimental results

In this section, the proposed ratio edge detector and the new referenceless estimator will be tested on both synthetic and real SAR images by using three state of the art denoising methods introduced for SAR images. All the experiments are done in MATLAB R2011a [29] and the parameters  $\alpha$ ,  $T_1$ ,  $T_2$  and  $T_3$  are set to 0.5, 0.1, 0.2 and 0.3 respectively.

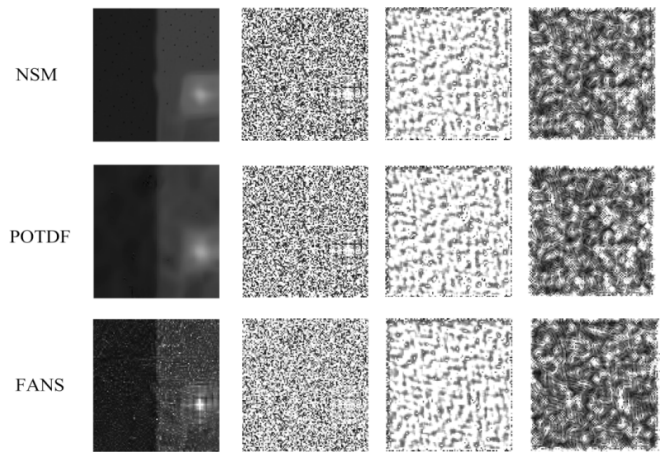


**Fig. 3. Left to right: First column: Denoised SAR Phantom images. Second: ratio images. Third: edges detected using ratio edge detector. Fourth: edges detected using enhanced ratio edge detector**

**Table 1. Objective evaluation of the denoised SAR Phantom image using different filters**

	Method		
	NSM	POTDF	FANS
PSNR (dB)	30.4585	30.1414	<b>31.6756</b>
ENL	<b>160.6319</b>	92.3553	5.5474
$\mu_{ratio}$	0.9628	0.9523	<b>0.9837</b>
$\beta_{ratio}$	0.5785	0.5478	<b>0.3564</b>
$\alpha\beta$	<b>0.6758</b>	0.6889	0.7501
$E - \alpha\beta$	0.5751	0.4433	<b>0.4251</b>

#### 4- 1- Synthetic data

In first set of experiments, the proposed estimator will be used to evaluate the synthetic image shown in Fig. 2 which is a 1-look 100×100 pixel image named SAR Phantom. The noisy SAR Phantom (Fig. 2-b) has simulated speckle with Gamma distribution with the mean value equal to 1. In addition, a strong scatter has been added to the image to evaluate the effectiveness of filters in maintaining it while denoising the image. Three state of the art filters named NSM [30], POTDF [31] and FANS [32], due to their excellent performance on despeckling SAR images are used to denoise the noisy SAR Phantom image. The denoised images using the three filters are shown in Fig. 3. In addition, the ratio image and also the edges detected using ratio edge detector and extended ratio edge detector algorithms for each method have also been shown in the same figure (left to right: second, third and fourth columns respectively). It is seen that enhanced ratio edge detector has detected more edges than the ratio edge detector algorithm. Although NSM and POTDF filters have efficiently suppressed the speckle, they have blurred the image and degraded the strong bright scatter while FANS has preserved it well at the cost of not suppressing the speckle. Comparing the ratio images, it is seen that in NSM and POTDF filtering, the scatter still exists which means having non-ideal filtering but in FANS the scatter is not available. Hence, it is too difficult to conclude which filter has better performance. To answer this question, six objective evaluating estimators

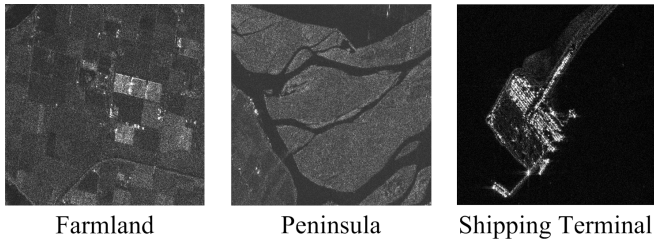


Fig. 4. Real SAR images from RADARSAT-1 data set used in experiments

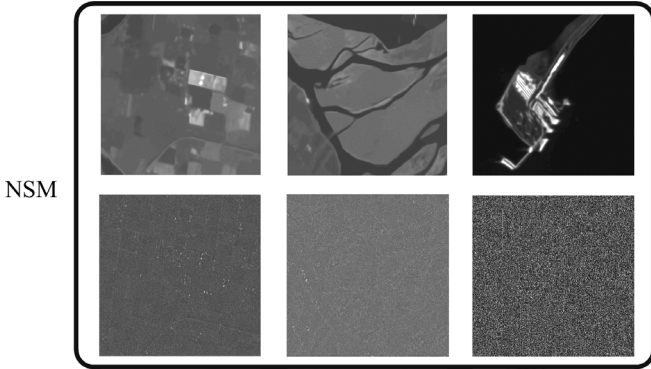


Fig. 5. The denoised real SAR images shown in Fig. 4 using NSM filter (first row) and their ratio images (second row)

named PSNR [20], ENL [17],  $\mu_{ratio}$  [25],  $\beta_{ratio}$  [25],  $\alpha\beta$  [25] and the proposed  $E - \alpha\beta$  are used and the obtained values are written in Table 1 (best results are bolded). To achieve ideal filtering, PSNR and ENL should be as high as possible,  $\mu_{ratio}$  equal to 1 and also  $\beta_{ratio}$ ,  $\alpha\beta$  and  $E - \alpha\beta$  equal to 0. Here, as it is seen the highest value for PSNR and  $\mu_{ratio}$  and the lowest values for  $\beta_{ratio}$  and  $E - \alpha\beta$  are obtained for FANS filter. Therefore, it has better edge preservation and filtering but the  $\alpha\beta$  estimator reports the lowest value for NSM filtering. In addition, FANS has the lowest ENL value meaning that less speckle rejection has been done while filtering the image. However, it should be noted that having higher ENL values does not really mean that the filtering operation is perfect. Although NSM and POTDF filters have higher ENL values than FANS, but as it is seen in Fig. 3, they

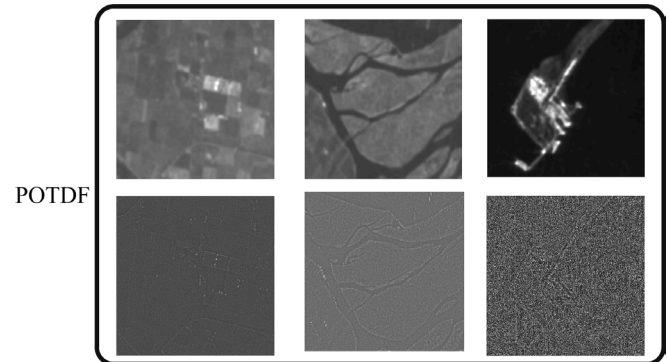


Fig. 6. The denoised real SAR images shown in Fig. 4 using POTDF filter (first row) and their ratio images (second row)

have blurred the image and completely destroyed the bright scatter. As it is shown, four out of six estimators (including the proposed  $E - \alpha\beta$ ) confirm that FANS has better results than the other filters. As far as the target is precisely evaluating real SAR images, this should be also tested on real SAR images, presented in the following.

#### 4- 2- Real SAR images

In this section, the experiments of Section 4.1 will be carried out on three real SAR images named Farmland, Peninsula and Shipping Terminal regions shown in Fig. 4 from the RADARSAT-1 dataset obtained from [33]. The raw data was collected in the Fine Beam 2 mode in June 16, 2002 and the radar was operating at C band with HH polarization. The filtered images of these three regions and also the ratio images are shown in Figs. 5, 6 and 7. In spite of all merits that the NSM and POTDF filters in speckle rejection have, it is seen that FANS filter outperforms these two filters in speckle rejection and edge preservation. In addition, it causes less blur effect to the filtered image. Comparing the ratio images, it is seen that there exist less geometrical contents in FANS filtered images while NSM and POTDF ratio images contain more geometrical contents. For objective evaluation, ENL,  $\mu_{ratio}$ ,  $\beta_{ratio}$ ,  $\alpha\beta$  and  $E - \alpha\beta$  are obtained for the filtered images and written in Table 2 (best results are bolded). Comparing the  $\mu_{ratio}$ ,  $\beta_{ratio}$  and  $E - \alpha\beta$  values obtained for

Table 2 Objective evaluation of the denoised real SAR images using different filters.

	Method and Region								
	NSM			POTDF			FANS		
	Farmland	Peninsula	Shipping Terminal	Farmland	Peninsula	Shipping Terminal	Farmland	Peninsula	Shipping Terminal
ENL	<b>582.8902</b>	<b>512.6365</b>	533.39	219.7694	169.5318	460.16	345.3554	264.1624	<b>10<sup>3</sup>×1.228</b>
$\mu_{ratio}$	0.6473	0.6691	0.6386	0.6619	0.6610	0.6578	<b>0.8783</b>	<b>0.8797</b>	<b>0.8823</b>
$\beta_{ratio}$	0.2162	0.6357	0.2489	0.2379	0.6368	0.3273	<b>0.1308</b>	<b>0.5218</b>	<b>0.1010</b>
$\alpha\beta$	<b>0.6893</b>	0.7295	<b>0.7949</b>	0.6918	<b>0.7207</b>	0.8069	0.7060	0.7344	0.8481
$E - \alpha\beta$	0.6585	0.6952	0.6973	0.6559	0.6887	0.7997	<b>0.6455</b>	<b>0.6726</b>	<b>0.6825</b>

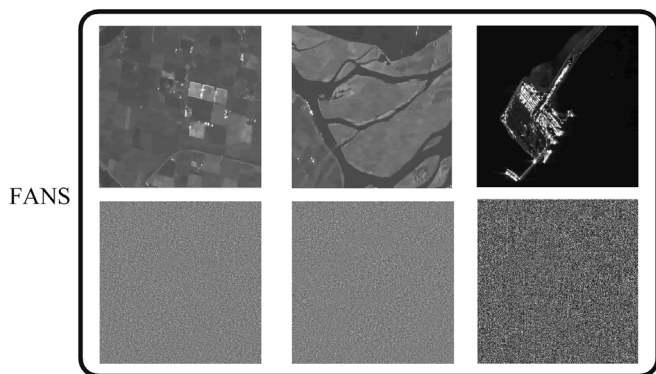


**Fig. 7. The denoised real SAR images shown in Fig. 4 using FANS filter (first row) and their ratio images (second row)**

these three regions, it is seen that these values confirm the subjective evaluation of the filtered images, since FANS has the best results due to these estimators. But the  $\alpha\beta$  estimator reports the NSM filtered image of Farmland and Shipping Terminal regions and POTDF filtered image of Peninsula region as the best edge preserved images. However, it is not true as they have lower  $\mu_{ratio}$  and higher  $\beta_{ratio}$  values than the FANS filtered one. Comparing the ENL values, it is seen that for NSM filtering, higher values are obtained except for the Shipping Terminal case where FANS filtered image has higher ENL value and the lowest values are for POTDF filtered images. From these results and also the results of SAR Phantom, it could be concluded that ENL is not really a good estimator to make conclusion on a filter performance. In addition, the  $\alpha\beta$  estimator fails to detect the best edge preserved image when using state of the art filtering methods which are very competitive to each other while  $E-\alpha\beta$  showed to be more effective in this case. So, the combination of  $\mu_{ratio}$ ,  $\beta_{ratio}$  and  $E-\alpha\beta$  estimators are recommended for denoised SAR image evaluation.

### 5- Conclusion

In this paper a new ratio edge detector algorithm named “Extended Ratio Edge Detector” and also a new estimator called “ $E-\alpha\beta$ ” were proposed which are the extended version of “Ratio Edge Detector” and “ $\alpha\beta$ ” algorithms. Experimental results on both synthetic and true SAR images showed that the extended ratio edge detector detects more edges in the ratio image than the ratio edge detector algorithm. In addition,  $E-\alpha\beta$  estimator proved to be more precise than  $\alpha\beta$ , when evaluating real SAR images using three competitive state of the art denoising algorithms, that were NSM, POTDF and FANS filters.

### 6- Acknowledgments

The authors would like to thank Dr. Bin Xu for providing NSM and POTDF and Dr. D. Cozzolino for providing FANS filter codes, and also Dr. L. Gomez for providing us the synthetic SAR Phantom image.

### References

[1] Preetha, C. Gorthi, S. and S. Mishra, D. Compressive Sensing Framework for Simultaneous Compression and Despeckling of SAR images, IEEE Eighth International Conference on Advances in Pattern Recognition (ICAPR), 15 (2015) 1-6.  
 [2] Xiao Feng Li, Ju Xu, Ji Jun Lou, Lijia Cao, Shengxiu

Zhang, Intensity image denoising for laser active imaging system using non-subsampled contourlet transform and SURE approach, Elsevier, Optik International Journal for Light and Electron Optics, 123(9) (2012) 808-813.

[3] O.V. Michailovich, A. Tannenbaum, Despeckling of medical ultrasound images IEEE Trans. On Ultrasonics, Ferroelectrics and Frequency Control, 53(1), (2006) 64-78.  
 [4] F. Chaillon, C. Fraschini, P. Courmontagne, Speckle noise reduction in SAS imagery Elsevier Journal of Signal Processing, 87(4) (2007) 762-781.  
 [5] F. Argenti, A. Lapini, T. Bianchi, A tutorial on speckle reduction in synthetic aperture radar images, IEEE Geoscience and Remote Sensing Magazine, 1(3) (2013) 6-35.  
 [6] J. Goodman, Some fundamental properties of speckle Journal of the Optical Society of America, 66 (1976) 1145-1150.  
 [7] T. R. Crimmins, Geometric filter for reducing speckle Optical Engineering, 25(5) (1986) 651-654.  
 [8] Y. Wu and H. Maitre, Smoothing speckled synthetic aperture radar images by using maximum homogenous region filters, Optical Engineering, 31(8) (1992) 1785-1792.  
 [9] F. Tupin, M. Sigelle, A. Chkeif and J-P Veran, Restoration of SAR images using recovery of discontinuities and non-linear optimization, In J. Van Leuween, G. Goos, J. Hartemis editor, EMMCVPR'97, Lecture notes in Computer Science, Springer, (1997).  
 [10] M. Koosha, K. Hajsadeghi and M. Koosha, Fine logarithmic adaptive soft morphological algorithm for synthetic aperture radar image segmentation, IET Journal of Image Processing, 8(2) (2014) 90-102.  
 [11] J. Bruniquel and A. Lopez, Analysis and enhancement of multi-temporal SAR data, Proc. SPIE 2315, Image and signal Processing for Remote Sensing, 342 (1994) doi:10.1117/12.196733.  
 [12] L. Rudin, P. L. Lions and S. Osher, Multiplicative denoising and deblurring: theory and algorithm, Geometric Level Sets in Imaging, Vision and Graphics, S.Osher and N.Paragios, Eds., Springer, (2003) 103-119.  
 [13] Z. Wang, X. Tan and Qi Yu, Sparse PDE for SAR image speckle suppression, IET Journal of Image Processing, 11(6) (2017) 425-432.  
 [14] G. Aubert and J. Aujol, A variational approach to removing multiplicative noise, SIAM J. Appl. Math., 68(4) (2008) 925-946.  
 [15] Y. Huang, M. Ng and Y. Wen, A new total variation method for multiplicative noise removal, SIAM J. Imag. Sci., 2(1) (2009) 20-40.  
 [16] J. M. Biocas-Dias and M. A. T. Figueiredo, Multiplicative noise removal using variable splitting and constrained optimization, IEEE Trans. Image Process., 19(7) (2010) 1720-1730.  
 [17] Yi Cui, Guangyi Zhou, Jian Yang and Yoshio Yamaguchi, Unsupervised estimation of the equivalent number of looks in SAR images, IEEE Geoscience and Remote Sensing Letters, 8(4) (2011) 710-714.

- [18] D. Brunet, E.R. Vrscay and Z. Wang, On the mathematical properties of the structural similarity index, *IEEE Transactions on Image Processing*, 21(4) (2011) 1488-1499.
- [19] A. Achim, E. Kuruoglu and J. Zerubia, SAR image filtering based on the heavy-tailed Rayleigh model, *Inst. Nat. Recherche Informat. Automatique (INRIA), France, Tech. Rep. 5493* (2005).
- [20] Q. Huynh-Thu, M. Ghanbari, Scope of validity of PSNR in image/video quality assessment, *IET, Electronic Letters*, 44(13) (2008) 800-801.
- [21] Haybert Markarian and Sedigheh Ghofrani, High-TV based CS framework using MAP estimator for SAR image enhancement, *IEEE Journal of Selected Topics in Applied Earth Observations and Remote Sensing*, 10(9) (2017) 4059-4073.
- [22] A. Buades, B. Coll and J. M. Morel, A review of image denoising algorithms with a new one, *SIAM Interdiscip. J. Multiscale Model. Simul.*, 4(2) (2005) 490-530.
- [23] L. Gomez et. al., Supervised constrained optimization of bayesian non-local means filter with sigma preselection for despeckling SAR images, *IEEE Trans. Geosci. Remote Sens.*, 51(8) (2013) 4563-4575.
- [24] S. Parrilli, M. Poderico, C. V. Angelino and L. Verdoliva, A nonlocal SAR image denoising algorithm base on LLMMSE wavelet shrinkage, *IEEE Trans. Geosci. Remote Sens.*, 50(2) (2012) 606-616.
- [25] L. Gomez, M. E. Buemi, J. C. Jacobo-Berlles and M. E. Mejail, A new image quality index for objectively evaluating despeckling filtering in SAR images, *IEEE Journal of Selected Topics in Applied Earth Observations and Remote Sensing*, 9(3) (2016) 1297-1307.
- [26] Xial Guang, Jiang Le, Jin Huang and Liu Jun, A fast high-order total variation minimization method for multiplicative noise removal, *Mathematical Problems in Engineering*, 2013 (2013) 13pages Article ID: 834035.
- [27] R. Touzi, A. Lopes and P. Bousquet, A statistical and geometrical edge detector for SAR images, *IEEE Trans. Image Process.*, 26(6) (1998) 764-773.
- [28] Y. Desnos and V. Matteini, Review on structure detection and speckle filtering on ERS-1 images, *EARSel adv. Remote Sens.* 2(2) (1993) 52-65, 1993.
- [29] Matlab, *The MathWorks*, 2011.
- [30] Bin Xu, Yi Cui, Zenghui Li and Jian Yang, An iterative SAR image filtering method using nonlocal sparse model, *IEEE Geoscience and Remote Sensing Letters*, 12(8) (2015) 1635-1639.
- [31] Bin Xu, Yi Cui, Zenghui Li, Bin Zuo, Jian Yang and Jianshe Song, Patch ordering based SAR image despeckling via transform domain filtering, *IEEE Journal of Selected Topics in Applied Earth Observations and Remote Sensing*, 8(4) (2015) 1682-1695.
- [32] D. Cozzolino, S. Parrilli, G. Scarpa, G. Poggi and L. Verdoliva, Fast adaptive nonlocal SAR despeckling, *IEEE Geoscience and Remote Sensing Letters*, 11(2) (2014) 524-528.
- [33] I. G. Cumming and F. H. Wong, *Digital Signal Processing of Synthetic Aperture Radar Data: Algorithms and Implementation*: Norwood, MA, USA: Artech House, (2004).

Please cite this article using:

H. Markarian and M. Nejati-Jahromi, A New Objective Evaluation Index for Despeckled SAR Images, *AUT J. Model.*

*Simul.*, 50(2) (2018) 141-146.

DOI: 10.22060/miscj.2018.14133.5091

